Hydroselenation of Simple Olefins: Elucidating the β-Selenium Radical Effect

Gabriel S. Phun,[b,‡] Hannah S. Slocumb,[b‡] Shaozhen Nie,[c] Kirsten J. Ruud,[b] Cheyenne Antonio,[d] Filipp Furche,[b*] Vy M. Dong,[b*] and Xiao-Hui Yang[a,e*]

[a]*Advanced Research Institute of Multidisciplinary Science, School of Chemistry and Chemical Engineering, Key Laboratory of Medical Molecule Science and Pharmaceutical Engineering, Ministry of Industry and Information Technology, Beijing Institute of Technology, Beijing, 100081, P. R. China*

[b]*Department of Chemistry, University of California, Irvine, Irvine, California, 92697, United States*

[c]*Department of Medicinal Chemistry, Glaxo-Smith-Kline, Collegeville, Pennsylvania, 19426, United States*

[d]*Department of Chemistry, University of California, San Francisco, San Francisco, California, 94143, United States*

[e]*State Key Laboratory of Elemento-Organic Chemistry, Nankai University, Tianjin, 300071, P. R. China.*

‡ These authors contributed equally to this work.

** Email: filipp.furche@uci.edu, dongv@uci.edu, xhyang@bit.edu.cn*

KEYWORDS: Selenides, Hydroselenation, Alkenes, Selenols, β-Seleno Effect, Diastereoselectivity

ABSTRACT: We report a light-promoted hydroselenation of alkenes with high *anti*-Markovnikov selectivity. Spectroscopic, kinetic, and computational mechanistic studies indicate that blue light activates an aryl diselenide to generate a seleno radical; this radical adds into an alkene to form a β-seleno carbon radical. Subsequent hydrogen atom transfer (HAT) generates the linear selenide with high selectivity in preference to the branched isomer. These studies reveal a unique β-selenium effect, where a selenide β to a carbon radical imparts high *anti*-selectivity for radical addition through delocalization of the HAT transition state.

While selenium is an element essential to life, its reactivity is less investigated relative to earlier chalcogens (oxygen and sulfur). Proteins containing selenocysteine (selenoproteins) are implicated in various essential antioxidant, redox, and metabolic processes. Selenoprotein thioredoxin reductase 1 catalyzes several antioxidant and redox processes via selenocysteine and cysteine residues through the formation and cleavage of a Se–S bond (Fig. 1A).[1] A disulfide bond between neighboring cysteines is generally conformationally unfavorable, but the use of selenocysteine makes the dichalcogen bond viable due to selenium's longer bond lengths.[2] Selenoproteins act as biomarkers for diseases including cancer and diabetes.[3] Recently, abnormal plasma levels of micronutrient selenium were found in patients suffering severe cases of COVID-19.[4] In addition to their use in nature, selenides have been incorporated into several drug targets.[5] Ethaselen is a potent thioredoxin reductase 1 inhibitor which has undergone phase I clinical trials (Fig. 1A).[6] Selenides are also effective ligands and catalysts; the Zhao lab has established a series of aryl selenide organocatalysts (Fig. 1A) that achieve a variety of stereoselective difunctionalizations.[7] In addition to catalysts, selenides often serve as alkyl radical precursors.[8] Alkyl selenides tend to exhibit higher stability in comparison to other radical precursors (e.g., halides)[9] and thus can be carried through multi-step syntheses toward impressive natural products.[10] Inoue and coworkers employed a phenyl selenide (Fig. 1A) to generate an alkyl radical in an elegant three-component coupling for the construction of resiniferatoxin.[10a] The selenide was synthesized from a less stable radical precursor which required several steps to access. The unique properties of Se have led to an interest in the development of methods to prepare organoselenides with hydroselenation being an especially attractive strategy.

Hydroselenation is an atom economical approach to add a Se–H bond across a C–C π-bond.[11] Several metal-catalyzed hydroselenations have been developed, mainly using activated alkenes (such as heterobicyclic alkenes,[12a] allenes,[12b] *N*-vinyl lactams,[12c] or α,β-unsaturated thioamides[12d]) or alkynes.[12] Our lab reported the Rh-catalyzed enantioselective

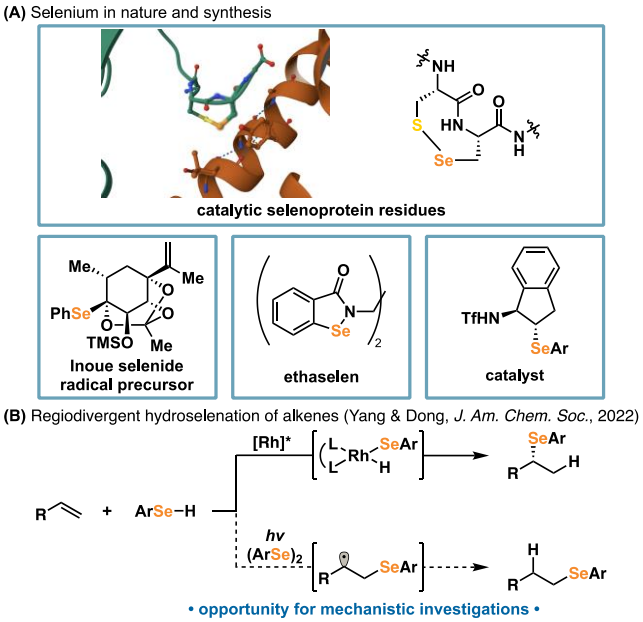

Figure 1. (A) Selenium in nature (catalytic residues in selenoprotein thioredoxin reductase 1) and synthesis (Inoue seleno radical precursor, ethaselen, and chiral catalyst). (B) Regiodivergent hydroselenation of alkenes via Rh (previous work) or light (proposed work).

hydroselenation of styrenes where we were able to access the Markovnikov-addition products with high stereoselectivity (Fig. 1B).[12e] In this follow up study, we aim to develop a complementary radical-mediated hydroselenation to form the *anti*-Markovnikov product. Previous studies have shown that seleno radicals can be generated photochemically. Ogawa reported a light-promoted hydroselenation of alkynes, proposing an alkenyl radical intermediate.[13] A number of other light-promoted reactions with selenides are known, including difunctionalizations,[14] couplings,[15] and cyclizations.[16] We imagined a light-generated seleno radical could add to the terminal position of an alkene to generate the more stable internal radical, which could then undergo HAT to give the *anti*-Markovnikov selenide (Fig. 1B). If successful, this approach would allow us to (1) access a complementary *anti*-Markovnikov motif, and (2) study the reactivity of the β-seleno radical by both experiment and theory. β-seleno radicals have been proposed in a number of seleno radical additions to alkenes for subsequent difunctionalizations.[14b–d, 17] An interesting observation amongst these reports is that these functionalizations often occur with high *anti*-selectivity, yet mechanistic studies of this phenomenon remain unexplored.

To access the *anti*-Markovnikov product by hydroselenation, we chose feedstock chemical styrene (1a) and commercially available benzeneselenol (2a) as our model system. The benzeneselenol sample contained 3 mol % diphenyl diselenide (3a) due to spontaneous selenol oxidative dimerization.[18] We observed no reactivity when the experiment was performed in the dark (Table 1, entry 1), however under ambient light we found that the hydroselenation can occur to give the *anti*-Markovnikov isomer 4aa in 15% yield and >20:1 *rr* (Table 1, entry 2). By shining blue LEDs on the reaction mixture and monitoring by TLC, we observed reaction completion and nearly quantitative yield of 4aa within 20 minutes (Table 1, entry 3). We suspected that the trace diphenyl diselenide 3 could be the photoactive species promoting reactivity.[13] Indeed, TLC monitoring indicated the reaction time could be shortened to five minutes by adding an additional 20 mol% of diphenyl diselenide (3a) (Table 1, entry 4). Together, these results support the critical role of blue light and catalytic diselenide in this coupling.

A condition-based sensitivity screen was performed as outlined by the Glorius group (Fig. 2).[19] Increased oxygen content lowered the yield by 26%. While high intensity of light showed similar results as the optimized conditions, low intensity afforded diminished yield (83%). Additionally, lower efficiency is observed at a larger reaction scale (20x optimized conditions, 69% yield).

Entry	Conditions	3a mol%	Time	Yield
1	dark	3	24 h	ND
2	ambient light	3	24 h	15%
3	blue LEDs	3	20 min	98%
4	blue LEDs	23	5 min	98%

Table 1. Optimization for the *anti*-Markovnikov hydroselenation of styrene using benzeneselenol. Yields are determined by NMR analysis using 1,3,5-trimethoxybenzene as the internal standard.

Synthetic Scope. We examined the light-promoted hydroselenation of twenty-eight different alkenes with benzeneselenol (2a) to generate the corresponding linear selenides (Fig. 2). High reactivity and regioselectivity (>20:1 *rr*) are obtained with mono-substituted alkenes (4aa–4av, 85–98% yield). Wide functional group tolerance is shown, including halides (4ab, 4ad, 4ae, 4ah), acids (4ak, 4ao), and heterocycles (4ar–4au). This process can occur with unactivated alkenes (4av), in contrast to the activated alkenes required in previous hydroselenations.[12a–e,20] Both 1,1-disubstituted (4aw–4ay, 90–94% yield) and 1,2-disubstituted alkenes (4az–4aab, 79–93% yield) undergo addition. A conjugated diene undergoes the selenol-ene to afford the homoallylic selenide (4aac) with 87% yield and >20:1 *rr*. We also applied this hydroselenation to prepare a Se-analogue of eletriptan, a migraine medication, which has an -SO_2Ph group instead of the SePh group in 4aad. The reaction gave a Se-analogue 4aad in a 31% yield. Several selenols (generated *in situ* from the diselenide and Ph_2POH) provide *anti*-Markovnikov products with high regioselectivity. A more electron-rich aryl selenol (4ba, 68% yield) shows higher reactivity compared to an electron-poor aryl selenol (4ca, 46% yield). A bulkier, less aromatic selenol had diminished reactivity (4da, 19% yield). Overall, this light promoted selenol-ene occurs under mild conditions to form linear organoselenides with excellent regiocontrol.

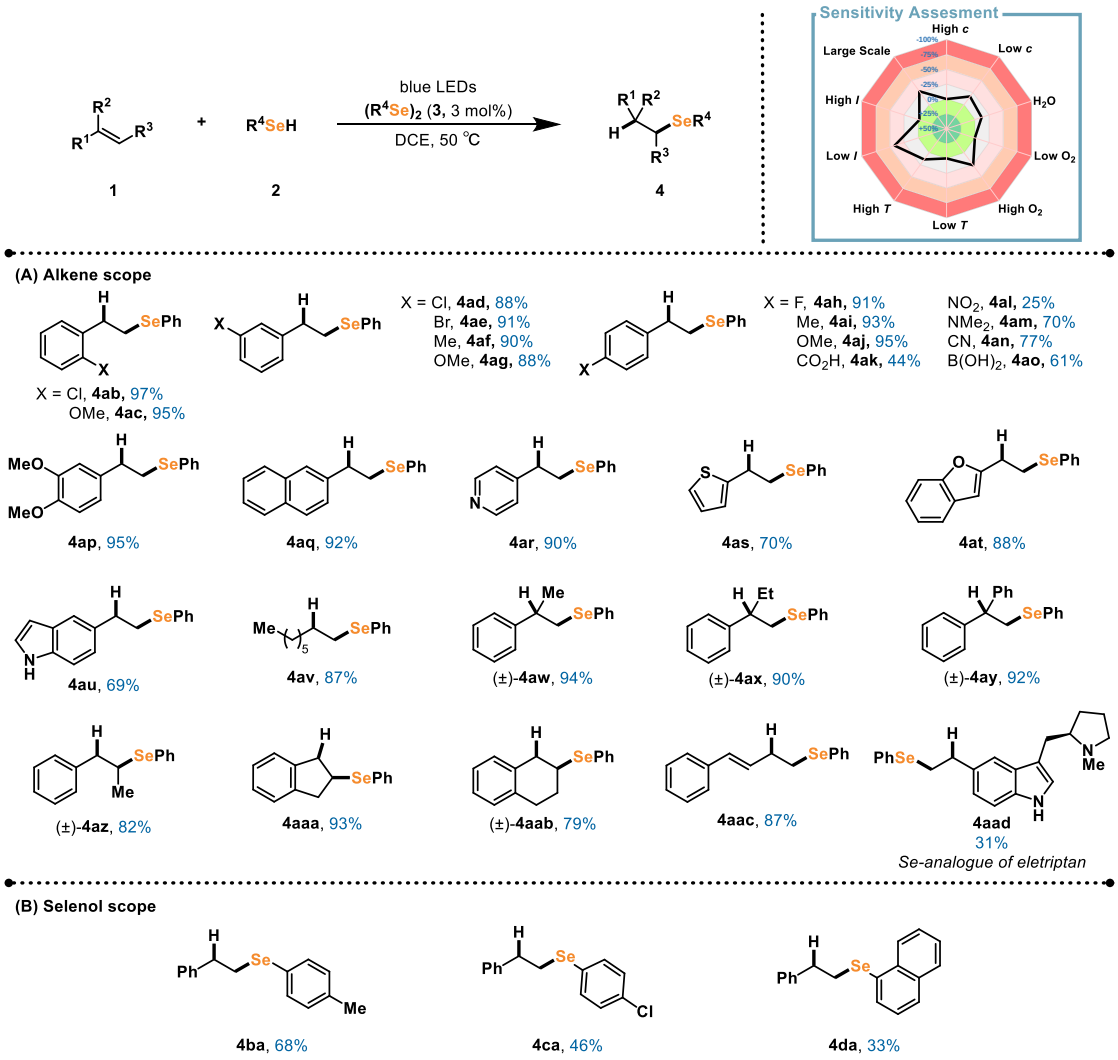

Figure 2. Scope of light-catalyzed hydroselenation for **(A)** alkenes and **(B)** selenols. Reaction conditions for alkene scope: **1** (1.0 equiv.), **2** (1.5 equiv.), 1,2-dichloroethane (0.25 M). Reaction conditions for selenol scope: **1** (1.0 equiv.), **3** (1.5 equiv.), Ph_2POH (1.5 equiv.), 1,2-dichloroethane (0.25 M). Reactions are run in a light box under blue LEDs and monitored by TLC for reaction completion (20 min–24 h). Temperature in the box rises to 50 ºC in 20 minutes due to LEDs and maintains that temperature over time. Regioselectivity determined by ^{1}H NMR analysis of the unpurified reaction mixture.

Mechanistic Hypotheses. Initially, we investigated the photoactive species of the transformation. UV-visible spectra showed that absorbance in the blue light region corresponds to diphenyl diselenide (Fig. S3). Ultra-fast transient absorption spectra also showed identical behavior between diphenyl diselenide (**3a**), the benzeneselenol sample (**2a**), and the reaction mixture (see SI 5.2 for details). Based on these spectroscopic results, we concluded that the photoactive species is diselenide (**3**), which is formed by selenols when exposed to light or oxygen.[18] Based on Ogawa's light-promoted hydroselenation of alkynes,[13] we were interested whether this selenol-ene involves radicals. We found that AIBN could be used as an initiator, giving 54% yield (Fig. 3A). The background reaction at 70 ºC gave only 15% yield, highlighting that AIBN effectively promotes hydroselenation. Additionally, a mixture of two distinct diselenides in DCE gave mixed diselenide product when exposed to blue LEDs (Fig. 3B). Thus, AIBN-mediated reactivity and crossover studies indicate the importance of seleno radicals in the reaction. A light-dark study (Fig. S6) revealed that light is necessary for reaction progress; when the light is off, the reactivity halts, but resumes when re-exposed to light. This is consistent with a previous report of high rates of recombination for seleno radicals.[17f]

Diselenide excitation is supported computationally (see SI 6.2). Excitation energies of **1a, 2a, 3a** and an optimized S_1 state geometry of **3a** were computed using time-dependent density functional theory (TDDFT) to support the feasibility of photoabsorption and photoinduced homolytic cleavage. The excitation energies are consistent with the experimental UV-visible spectra, with **3a** being the only species with a S_1 excitation within range of the blue LEDs. The S_1 state of **3a** has Se–Se σ* character. Upon S_1 state geometry optimization, the Se–Se bond lengthens by 0.47Å. Moreover, the computed Se–Se bond dissociation energy changes from energetically unfavorable (35.7 kcal/mol) to favorable (-15.3 kcal/mol) upon S_1 excitation.

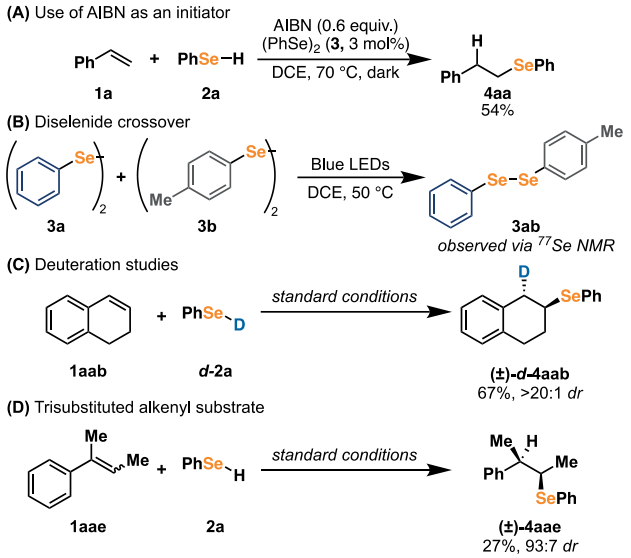

Figure 3. (A) Reaction run in the dark using AIBN as an initiator; (B) Diselenide crossover experiment; (C) *Anti*-selective addition of a deuterated selenol to a cyclic styrene; (D) *Anti*-selective addition of selenol to a trisubstituted styrene.

Deuterium labeling studies revealed high *anti*-selectivity for cyclic selenide **4aab** (Fig. 3C). Similarly, hydroselenation of a tri-substituted acyclic alkene gave high selectivity for a single diastereomer for selenide **4aae** (Fig. 3D). High diastereoselectivity is relatively uncommon in radical reactions, so we investigated several potential mechanisms to determine which reflected the observed selectivity.

The importance of diphenyl diselenide and light in the reaction suggests activation of the diselenide **3** by light (Fig. 4). Excited state diselenide **3*** can undergo homolytic bond cleavage to form seleno radical **I**. Based on literature precedence,[13] we propose that the radical could then add to alkene **1** to form C-radical **II**. To investigate the origin of *anti*-selectivity from this β-seleno radical, we proposed three diverging mechanisms: **M1**, a diastereoselective hydrogen atom transfer (HAT); **M2**, a seleniranium process; and **M3**, a radical seleniranium process. Two other mechanisms, involving a Dexter Energy Transfer (DET) event or formation of a styrene radical cation were also investigated, but these mechanisms favored *syn*-addition and were therefore ruled out (see SI for details). We found that **M1** (Fig. 4) is the most likely mechanism, and we herein detail our experimental and computational results which support or refute **M1**, **M2**, and **M3**.

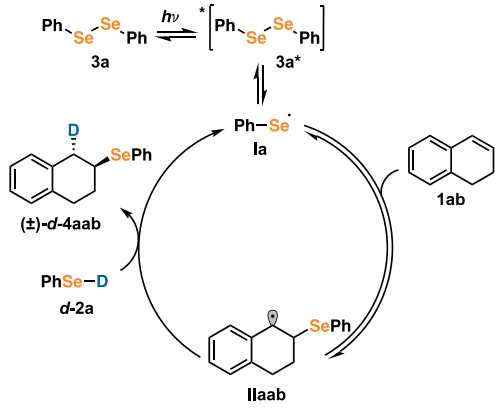

Figure 4. Favored mechanism for diastereoselective formation of ***d*-4aab**.

Selective HAT mechanism (M1). For **M1** (Fig. 4), seleno radical **Ia** adds to the alkene **1ab** to form alkyl radical **IIaab**. A subsequent HAT with selenol *d*-**2a** provides product **4aab**. Ogawa has proposed a similar mechanism where the homolytic bond cleavage of diselenides generates seleno radicals, which undergo addition to alkynes.[13] This mechanism is in accordance with the experimental observation of seleno radicals, but to probe whether the predicted diastereoselectivity reflected the experimental results we turned to computational studies.

Computational Studies of M1. We focused our computational studies on analyzing the predicted selectivity for cyclic styrene substrate **1ab**. For **M1**, the diastereo-determining step will be the HAT step; hence we focused on the calculations for the intermediate (**IIaab**), transition state (**TS2**) and product (**4aab**) for that step.

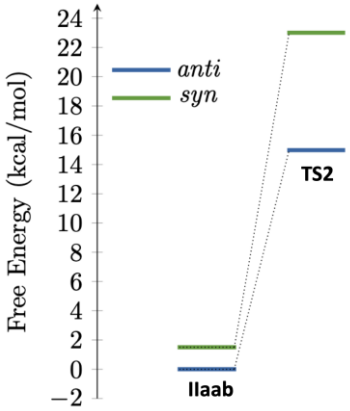

Figure 5. Energies of the intermediate **IIaab** and HAT transition state (**TS2**) for *syn*- and *anti*-addition. Energies are: **IIaab**-*anti*, 0 kcal/mol; **IIaab**-*syn*, 1.51 kcal/mol; **TS2**-*anti*, 14.98 kcal/mol; **TS2**-*syn*, 23.01 kcal/mol.

Relative free energies of transition states and intermediates were computed with DFT to predict the diastereomeric ratios (*dr*) (Fig. 5). It is likely that there is interconversion between the *anti*- and *syn*- isomers of **IIaab**, due to the low barrier of inversion for tetrahedral C-radicals. This is the condition for Curtin-Hammett control which results in a *dr* that only depends on the transition state free energies rather than the activation energies. The computed *anti*- to *syn*-product ratio is >99:1 *dr*, which corresponds well with the experimentally observed >20:1 *dr*. In the less likely scenario where there is not facile interconversion of *anti*- and *syn*-**IIaab**, the reaction would be under kinetic control and therefore depend upon the ΔΔG between *anti*- and *syn*-**IIaab**. In this case, calculations also indicate a >99:1 *dr*, still supporting experimental results.

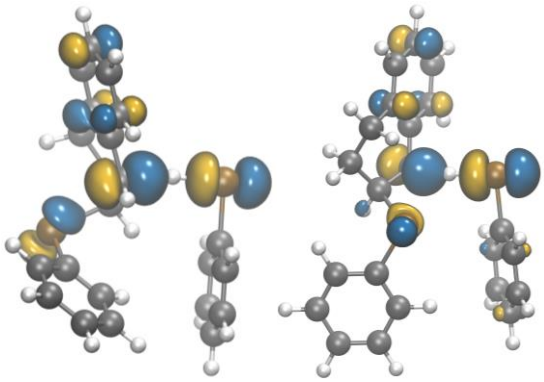

Figure 6. SOMO of the *anti* and *syn* HAT transition states (**TS2**).

Comparing the SOMOs of the HAT step transition state (**TS2**) reveals a qualitative difference between the *syn*- and *anti*-**TS2** electron densities (Fig. 6). The SOMO of the *anti*-**TS2** is delocalized a greater distance because selenium atoms are more linear. The SOMO of both transition state structures has weak C–H bonding and Se–H antibonding character (Fig. 6). However, the almost linear (133º) Se–C–C configuration over 5.5 Å in the *anti*-**TS2** structure affords additional stabilization of the SOMO by hyperconjugation with the σ* orbital of the adjacent C–Se bond, whereas the 77º Se–C–C angle reduces the length scale of delocalization (3.74 Å) in the *syn*-**TS2** structure. The *anti*-**TS2** SOMO delocalization shows some antibonding character and results in a small lengthening in the *anti*-**TS2** β-Se–C bond (2.005 Å) compared to the *syn*-**TS2** β-Se–C bond (2.003 Å). Based on these results, it is likely that electronic effects contribute greatly to give the high *anti*-selectivity. Sterics may also have an impact,[17l] however would not explain the observed bond lengthening and extended delocalization.

We were also interested in the high diastereoselectivity observed for acyclic product **4aae**. DFT calculations were performed on the entire reaction coordinate (see SI). Calculations indicated a high *anti*-selectivity in this case as well. However, both (*E*)- and (*Z*)-**1ae** give the same diastereomer experimentally, which was found to be the product of *anti*-addition to (*E*)-**1ae**. Depletion of (*E*)-**1ae** occurs more quickly in the reaction, and isomerization between the two alkenes under reaction conditions is also observed. Thus, it is possible that there is a pre-equilibrium between the alkenes followed by a faster *anti*-addition reaction to (*E*)-**1ae**. The calculations do not fully describe a significantly faster reaction with (*E*)-**1ae**, but do support high *anti*-selectivity in a similar fashion to the cyclic system.

Based on our observed diastereoselectivity and computational investigations, we propose a novel "β-selenium effect" for radical additions due to delocalization of the transition state SOMO. This effect is an exciting parallel to the β-silicon effect.[21] Further, our present results suggest that the β-selenium effect arises from delocalization rather than a seleniranium intermediate.[22]

We were interested in whether the β-selenium effect extends to other radical additions, so we investigated whether the C-radical can be trapped using H_2O_2. We found that a mixture of alkene **1ab**, **3a**, and H_2O_2 gave sole *anti*-addition (Scheme 1).

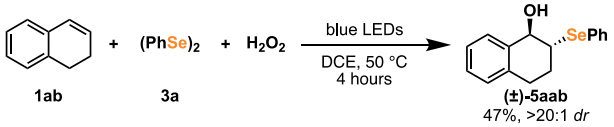

Scheme 1. Use of H_2O_2 as a radical trap.

From these studies, we conclude that the β-selenium effect is applicable to trapping of C-radicals β to a selenide with high stereocontrol.

Seleniranium mechanism (M2). Mechanisms involving seleniraniums are well precedented.[23] The addition of an electrophilic selenium moiety to an alkene forms a seleniranium, which can subsequently be opened by a range of nucleophiles. Addition of the nucleophile occurs with *anti*-selectivity. This reactivity includes applications such as polyene cyclizations,[23b] selenoetherifications[24] and selenolactonizations.[25] Strong evidence for seleniraniums has been observed, as the seleniranium ion structure has recently been thoroughly characterized.[26] Based on this literature precedence and the observed *anti*-selectivity, we were curious whether our selenolene occurs *via* a seleniranium intermediate. In this proposed mechanism (Fig. 7), C-radical intermediate **IIaab** can be oxidized to form seleniranium intermediate **IIIaab**. Subsequent hydrogen atom abstraction (HAT) and reduction can give the product **4aab** and regenerate seleno radical **Ia**. To probe this mechanism, we imagined independently synthesizing a seleniranium and subjecting it to the reaction conditions, but the instability of seleniraniums precluded their use at reaction temperature.[24b, 26]

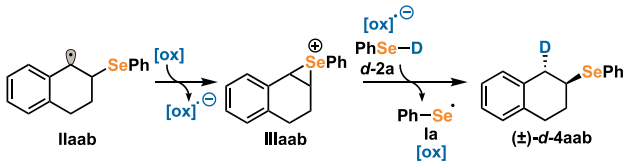

Figure 7. Proposed radical seleniranium mechanism (**M2**) for formation of *anti*-***d*-4aab** starting from carbon radical **IIaab.**

To form the seleniranium, oxidation is required and so, we investigated the presence of oxidants in the reaction. There are two possible mechanisms for oxidation: first, C-radical **II** can be oxidized to form a carbocation followed by ring closing to form **III** (Fig. 8A), or ring closing can occur first to form the radical selenirane **IV** followed by oxidation to form **III** (Fig. 8B).

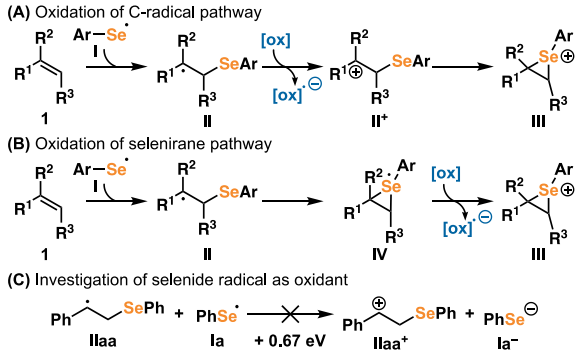

Figure 8. (A) Oxidation pathway involving carbocation; (B) oxidation pathway involving selenirane; (C) investigated oxidation of C-radical.

Based upon previous redox studies of benzeneselenol, styrene, and diphenyl diselenide, we realized that the ground state species of these reagents were unable to facilitate oxidation.[27] Therefore, we calculated the redox potentials of various excited-state species in the reaction. The 1e- reduction potential for seleno radical **Ia** is calculated to be -4.46 eV. For the carbocation pathway (Fig. 8A), the oxidation of the C-radical intermediate **IIaa** is +5.13 eV (Table 2). Based on these calculations, the redox event using a seleno radical **Ia** as an oxidant for **IIaa** is energetically uphill and therefore unlikely (Fig. 8C). DFT studies of the neutral selenirane radical indicated that this was not an energetically feasible intermediate (*vide infra*).

	Ia → Ia$^{\bullet-}$	**IIaa → IIaa^{+}**
Adiabatic Electronic Energy Difference	-4.46 eV	5.13 eV

Table 2. Energy differences for redox processes of radical intermediates.

To investigate whether oxygen could be the oxidant, parallel experiments were run: one under inert conditions (<5.0 ppm O_2), one under brief exposure to the atmosphere, and one under an O_2 balloon. All three reactions proceeded similarly, and the reaction occurred in the absence of O_2; therefore, we concluded that O_2 is unlikely to affect reactivity (Table 3).

	Inert	**Air**	**O_2 balloon**
Yield (µmol)	72.1 ± 4.5	73.2 ± 4.6	74.4 ± 4.6

Table 3. NMR yields of product after three minutes using triphenylmethane as internal standard. Reaction conditions: **1a** (0.1 mmol), **2a** (0.15 mmol), solvent (0.167 M), blue LED irradiation for five minutes.

Further, we investigated the impact of solvent dielectric constant on reaction rate. Based on Marcus theory,[28] if redox reactivity occurred to form a seleniranium, the reaction should be faster in solvents with higher dielectric constants. A higher solvent dielectric constant allows for rapid solvent reorganization upon charged species formation. However, we observed no correlation between solvent dielectric constant and yield at an early time point in the reaction (Fig. 9). In fact, acetonitrile, which has the highest dielectric constant and smallest radius, led to one of the lowest yields early in the reaction. Therefore, it is unlikely that charged species formation occurs during this reaction.

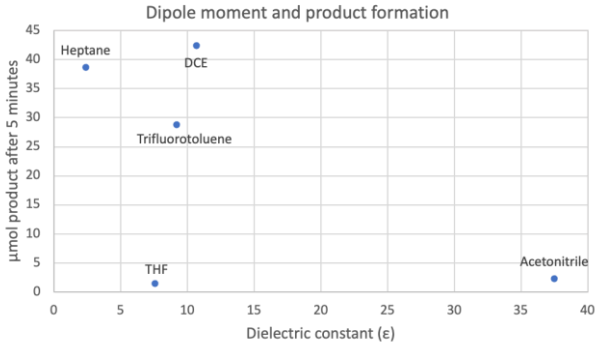

Figure 9. Observed lack of trend between dielectric constant and product formation early in the reaction. Tested solvents included heptane, 1,2-dichloroethane, α,α,α-trifluorotoluene, tetrahydrofuran, and acetonitrile. Reaction conditions: **1a** (0.1 mmol), **2a** (0.15 mmol), solvent (0.25 M), blue LED irradiation for five minutes. Yield measured using GCFID analysis with trimethoxybenzene as internal standard.

Based on these mechanistic studies, we were able to conclude that the presence of oxidants and ionized intermediates is unlikely. Therefore, a seleniranium mechanism for this reaction is improbable.

Selenirane mechanism (M3). After establishing **M2** is unlikely, we imagined a similar mechanism involving a neutral selenirane (Fig. 10).

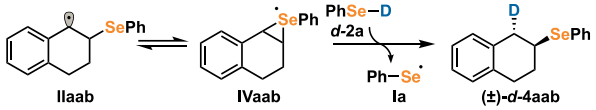

Figure 10. Proposed radical selenirane mechanism (**M3**) for formation of *anti*-***d*-4aab** starting from carbon radical **IIaab**.

In this mechanism, C-centered radical **IIaab** could be in equilibrium with the Se-centered radical selenirane **IVaab**, and could undergo HAT with selenol **2a** to give the product **4aab** and regenerate seleno radical **Ia**. This pathway would similarly have high *anti*-selectivity but would not require redox activity. We investigated **M3** computationally to determine the energetic feasibility. A potential energy surface scan of **VI** (Fig. 11) varying the Se–C1 and Se–C2 bond lengths showed no local minimum that corresponded to the selenirane ring and no saddle points that would correspond to a transition state (Fig. 11). The lack of energetically feasible intermediates or transition states for a radical selenirane indicates that **M3** is unlikely to be the operative mechanism.

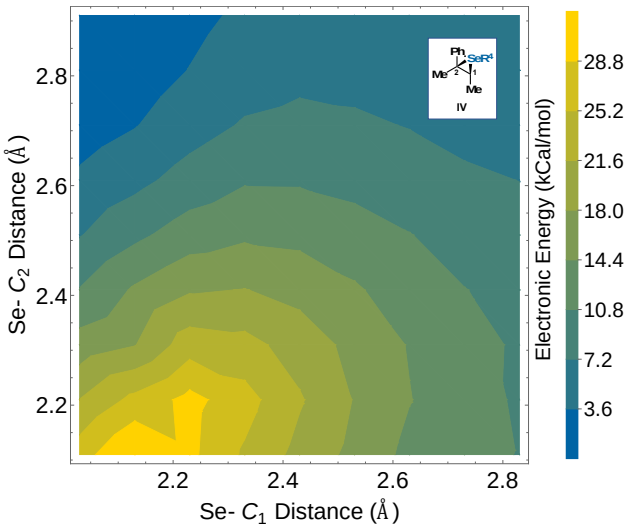

Figure 11. Potential energy surface scan of selenirane mechanism. No minima (intermediates) or saddle points (transition states) were found corresponding to a selenirane.

Conclusion. The generation of carbon radicals from alkenes is an exciting approach to hydrofunctionalization. This strategy can be achieved through (1) metal-hydride hydrogen atom transfer (MHAT);[29] (2) generation of radical cations from alkenes;[30] or (3) the addition of a heteroatom radical to alkenes.[31] We report a novel hydroselenation falling under this third approach, where a selenide radical adds to an alkene. Using blue LEDs, we were able to access novel selenides. The transformation proceeds with a variety of substrates, including unactivated alkenes and drug-like molecules. The exploration of several potential mechanisms (Table 4) led us to identify a mechanism involving a C-radical as the most likely pathway (**M1**).

		M1	**M2**	**M3**
Experimental Evidence	***anti*-addition**	✓	✓	✓
	Radical evidence	✓	✓	✓
	No rate correlation with polarity of solvent	✓	X	✓
Computational Evidence	**Energetically Feasible**	✓	X	✓
	Found Transition States	✓	N/A	X
	Favors *anti*-addition	✓	✓	✓

Table 4. Summary of investigated mechanisms and their agreement or disagreement with experimental and computational results.

Through computational studies, we have been able to identify a novel β-selenium effect which leads to high *anti*-selectivity for trapping C-radicals β to a selenide. In previous studies, sterics have been proposed to impact selectivity of addition to β-carbon radicals; however, through computational studies we have been able to elucidate additional electronic factors which play a significant role in selectivity. This relatively strong stereoelectronic effect appears to be caused by the much greater energetic accessibility of C–Se σ* orbitals compared to other C–X σ bonds with second-row elements. We hope that the application of the β-selenium effect can aid in future stereoselective syntheses, and we expect insights from this study will help to guide future work in hydroselenation and functionalization of selenides.

Methods.

Computational methods. All calculations were performed using Turbomole.[32] The molecular geometries were optimized using the DFT functional PBE0,[33] the triple ζ quality def2-TZVP basis set,[34] resolution-of-the-identity approximation (RI),[35] D3 dispersion corrections,[36] and COSMO with a dielectric constant of 10.45 corresponding to DCE.[37] GKS-RPA[38] single point calculations using the DFT functional PBE were then done on these optimized geometries and adiabatic electronic energies using the resolution-of-identity random phase approximation (RI-RPA),[39] 60 frequency quadrature points, triple ζ quality def2-TZVP basis set, an SCF convergence threshold of 10^{-8} Hartree, and the 6 grids for functional integrations. Finally, the free energy corrections were computed using the "Thermo submodule" of xTB.[40]

Experimental methods.

Alkene scope. In a N_2-filled glovebox, benzeneselenol (2a, 0.15 mmol, 1.5 equiv.) containing 3 mol% diphenyl diselenide (3a) was added to a solution of alkene (1, 0.1 mmol, 1.0 equiv.) in DCE (0.40 mL) in a 1-dram vial. The vial was sealed with a septa cap and brought out from glovebox. During irradiation with blue LEDs, the temperature was allowed to rise due to proximity to the lights, maintaining ~50 ºC after 20 minutes. The reaction mixture was monitored by TLC, and reactions were irradiated until starting material was consumed or the reaction stalled (1–24 h). The resulting mixture was then cooled to room temperature and the solvent was evaporated by rotary evaporation. The regioselectivities were determined by ^{1}H NMR analysis of the unpurified reaction mixture. Isolated yields (obtained by preparative TLC) are reported.

Selenol scope. In a N_2-filled glovebox, diselenide (3, 0.15 mmol, 1.5 equiv.) and diphenylphosphine oxide (0.15 mmol, 1.5 equiv.) were weighed in a 1-dram vial. A mixture of diselenide and diphenylphosphine oxide forms selenol *in situ*.[9] DCE (0.40 mL) and styrene (1a, 0.1 mmol, 1.0 equiv.) were added. The vial was sealed with a septa cap and brought out from glovebox. During irradiation with blue LEDs, the temperature was allowed to rise due to proximity to the lights, maintaining ~50 ºC after 20 minutes. The reaction mixture was monitored by TLC, and reactions were irradiated until starting material was consumed or the reaction stalled (1–24 h). The resulting mixture was then cooled to room temperature and the solvent was evaporated by rotary evaporation. The regioselectivities were determined by ^{1}H NMR analysis of the unpurified reaction mixture. Isolated yields (obtained by preparative TLC) are reported.

ASSOCIATED CONTENT

Supporting Information

The Supporting Information is available free of charge on the ChemRxiv website.

Experimental procedures and spectral data for all new compounds (PDF)

AUTHOR INFORMATION

Corresponding Author

Prof. Xiao-Hui Yang - Advanced Research Institute of Multidisciplinary Science, and School of Chemistry and Chemical Engineering, Beijing Institute of Technology, Beijing100081, China; Email: xhyang@bit.edu.cn
Prof. Vy Dong - Department of Chemistry, University of California, Irvine, Irvine, California92697, United States; https://orcid.org/0000-0002-8099-1048;
Prof. Filipp Furche - University of California, Irvine, Department of Chemistry, 1102 Natural Sciences II, Irvine, CA 92617-2025, USA; https://orcid.org/0000-0001-8520-3971

Author Contributions

‡These authors contributed equally.

Funding Sources

X.-H.Y. thanks the National Natural Science Foundation of China (Nos. 22371016 and 22201018), Beijing Natural Science Foundation (No. 2222024), and the National R&D Program of China (No. 2021YFA1401200) for funding. V.M.D. thanks the U.S. National Science Foundation (No. CHE-1956457) and National Institutes of Health (5R35GM127071-05) for funding. H.S.S. thanks the National Science Foundation Graduate Research Fellowship (No. DGE-1839285). G.S.P. thanks the U.S. Department of Energy, Office of Basic Energy Sciences, under Award Number DE-SC0018352.

Notes

The authors declare no competing financial interest.

ACKNOWLEDGMENT

We thank Dr. Dmitry Fishman for his work on the transient absorption spectroscopy. We also thank the UCI mass spectroscopy facility for their work on the high resolution mass spectroscopy data.

REFERENCES

1. (a) Cheng, Q.; Sandalova, T.; Lindqvist, Y.; Arnér, E. S. J. Crystal Structure and Catalysis of the Selenoprotein Thioredoxin Reductase 1. *J. Biol. Chem.* **2009**, *284* (6), 3998–4008. DOI: 10.1074/JBC.M807068200 (b) Cheng, Q.; Sandalova, T.; Lindqvist, Y.; Arnér, E. S. J. Crystal Structure of Recombinant Rat Selenoprotein Thioredoxin Reductase 1 with Oxidized C-Terminal Tail. *RCSB PDB*. 2008. DOI: 10.2210/pdb3EAO/pdb (PDB ID: 3EAO)

2. Gromer, S.; Johansson, L.; Bauer, H.; Arscott, L. D.; Rauch, S.; Ballou, D. P.; Williams, C. H.; Schirmer, R. H.; Arnér, E. S. J. Active Sites of Thioredoxin Reductases: Why Selenoproteins? *Proc. Natl. Acad. Sci. USA* **2003**, *100* (22), 12618–12623. DOI: 10.1073/pnas.2134510100

3. Roman, M.; Jitaru, P.; Barbante, C. Selenium Biochemistry and Its Role for Human Health. *Metallomics* **2013**, *6* (1), 25–54. DOI: 10.1039/C3MT00185G

4. (a) Moghaddam, A.; Heller, R. A.; Sun, Q.; Seelig, J.; Cherkezov, A.; Seibert, L.; Hackler, J.; Seemann, P.; Diegmann, J.; Pilz, M.; Bachmann, M.; Minich, W. B.; Schomburg, L. Selenium Deficiency Is Associated with Mortality Risk from COVID-19. *Nutrients* **2020**, *12* (7), 2098. DOI: 10.3390/NU12072098. (b) Alkattan, A.; Alabdulkareem, K.; Kamel, A.; Abdelseed, H.; Almutairi, Y.; Alsalameen, E. Correlation between Micronutrient Plasma Concentration and Disease Severity in COVID-19 Patients. *Alexandria J. Med.* **2021**, *57* (1), 21–27. DOI: 10.1080/20905068.2020.1870788.

5. For select reviews, see: (a) Chuai, H.; Zhang, S. Q.; Bai, H.; Li, J.; Wang, Y.; Sun, J.; Wen, E.; Zhang, J.; Xin, M. Small Molecule Selenium-Containing Compounds: Recent Development and Therapeutic Applications. *Eur. J. Med. Chem.* **2021**, *223*, 113621. DOI: 10.1016/J.EJMECH.2021.113621(b) Radomska, D.; Czarnomysy, R.; Radomski, D.; Bielawski, K. Selenium Compounds as Novel Potential Anticancer Agents. *Int. J. Mol. Sci.* **2021**, *22*, 1009– 1035, DOI: 10.3390/ijms22031009 (c) Ali, W.; Benedetti, R.; Handzlik, J.; Zwergel, C.; Battistelli, C. The innovative potential of selenium-containing agents for fighting cancer and viral infections. *Drug Discovery Today* **2021**, *26*, 256– 263, DOI: 10.1016/j.drudis.2020.10.014 (d) Gandin, V.; Khalkar, P.; Braude, J.; Fernandes, A. P. Organic selenium compounds as potential chemotherapeutic agents for improved cancer treatment. *Free Radic. Biol. Med.* **2018**, *127*, 80– 97, DOI: 10.1016/j.freeradbiomed.2018.05.001 (e) Fernandes, A. P.; Gandin, V. Selenium compounds as therapeutic agents in cancer. *Biochim. Biophys. Acta* **2015**, *1850*, 1642– 1660, DOI: 10.1016/j.bbagen.2014.10.008

6. (a) Wang, L.; Yang, Z.; Fu, J.; Yin, H.; Xiong, K.; Tan, Q.; Jin, H.; Li, J.; Wang, T.; Tang, W.; Yin, J.; Cai, G.; Liu, M.; Kehr, S.; Becker, K.; Zeng, H. Ethaselen: A Potent Mammalian Thioredoxin Reductase 1 Inhibitor and Novel Organoselenium Anticancer Agent. *Free Radic. Biol. Med.* **2012**, *52* (5), 898–908. DOI: 10.1016/J.FREERADBIOMED.2011.11.034 (b) Zheng, X.; Chen, Y.; Bai, M.; Liu, Y.; Xu, B.; Sun, R.; Zeng, H. The Antimetastatic Effect and Underlying Mechanisms of Thioredoxin Reductase Inhibitor Ethaselen. *Free Radic. Biol. Med.* **2019**, *131*, 7–17. DOI: 10.1016/J.FREERADBIOMED.2018.11.030

7. For a review, see: (a) Liao, L.; Zhao, X. Indane-Based Chiral Aryl Chalcogenide Catalysts: Development and Applications in Asymmetric Electrophilic Reactions. *Acc. Chem. Res.* **2022**, *55* (17), 2439–2453. DOI: 10.1021/ACS.ACCOUNTS.2C00201/ASSET/IMAGES/LARGE/AR2C00201_0021.JPEG. For select examples, see: (b) Liu, X.; Liang, Y.; Ji, J.; Luo, J.; Zhao, X. Chiral Selenide-Catalyzed Enantioselective Allylic Reaction and Intermolecular Difunctionalization of Alkenes: Efficient Construction of C-SCF_3 Stereogenic Molecules. *J. Am. Chem. Soc.* **2018**, *140* (14), 4782–4786. DOI: 10.1021/jacs.8b01513 (c) Liang, Y.; Zhao, X. Enantioselective Construction of Chiral Sulfides via Catalytic Electrophilic Azidothiolation and Oxythiolation of N-Allyl Sulfonamides. *ACS Catal.* **2019**, *9* (8), 6896–6902. DOI: 10.1021/acscatal.9b01900 (d) Zhang, Y.; Liang, Y.; Zhao, X. Chiral Selenide-Catalyzed, Highly Regio- And Enantioselective Intermolecular Thioarylation of Alkenes with Phenols. *ACS Catal* **2021**, *11* (6), 3755–3761. DOI: 10.1021/acscatal.1c00296

8. (a) Pandey, G.; Sesha, K S; Rao, P.; Soma Sekhar, B. B. V. Photosensitized One-Electron Reductive Cleavage of a Carbon-Selenium Bond: A Novel Chemoselective Deselenenylation and Phenylselenenyl Group Transfer Radical Chain Reaction. *J. Chem. Soc., Chem. Commun.* **1993** *21*, 1636–1638. DOI: 10.1039/C39930001636 (b) Pandey, G.; Sesha Poleswara Rao, K. S.; Nageshwar Rao, K. V. Photosensitized Electron Transfer Promoted Reductive Activation of Carbon-Selenium Bonds to Generate Carbon-Centered Radicals: Application for Unimolecular Group Transfer Radical Reactions. *Journal of Organic Chemistry* **1996**, *61* (20), 6799–6804. DOI: 10.1021/jo960805i (c) Renaud, P. Radical Reactions Using Selenium Precursors. **2000**, 81–112. DOI: 10.1007/3-540-48171-0_4

9. Bowman, W. R. Selenium Compounds in Radical Reactions. *Organoselenium Chemistry: Synthesis and Reactions* **2011**, 111–146. DOI: 10.1002/9783527641949.CH3

10. (a) Hashimoto, S.; Katoh, S. I.; Kato, T.; Urabe, D.; Inoue, M. Total Synthesis of Resiniferatoxin Enabled by Radical-Mediated Three-Component Coupling and 7-Endo Cyclization. *J. Am. Chem. Soc.* **2017**, *139* (45), 16420–16429. DOI: 10.1021/jacs.7b10177 (b) Clive, D. L. J.; Tao, Y.; Khodabocus, A.; Wu, Y.-J.; Gae'tan Angoh, A.; Bennett, S. M.; Boddy, C. N.; Bordeleau, L.; Kellner, D.; Kleiner, G.; Middleton, D. S.; Nichols, C. J.; Richardson, S. R.; Vernon, P. G. Total Synthesis of Crystalline (±)-Fredericamycin A. Use of Radical Spirocyclization. *J. Am. Chem. Soc* **1994**, *116*, 11275–11286. DOI: 10.1021/ja00104a009 (c) Hirose, A.; Watanabe, A.; Ogino, K.; Nagatomo, M.; Inoue, M. Unified Total Syntheses of Rhamnofolane, Tigliane, and Daphnane Diterpenoids. *J Am Chem Soc* **2021**, *143* (31), 12387–12396. DOI: 10.1021/jacs.1c06450 (d) Yuan, P.; Gaich, T. Enantioselective Total Synthesis of (+)-Pepluanol A. *Org Lett* **2022**, *24* (26), 4717–4721. DOI: 10.1021/ACS.ORGLETT.2C00961 (e) Asaba, T.; Katoh, Y.; Urabe, D.; Inoue, M. Total Synthesis of Crotophorbolone. *Angewandte Chemie International Edition* **2015**, *54* (48), 14457–14461. DOI: 10.1002/ANIE.201509160 (f) Zi, W.; Xie, W.; Ma, D. Total Synthesis of Akuammiline Alkaloid (-)-Vincorine via Intramolecular Oxidative Coupling. *J Am Chem Soc* **2012**, *134* (22), 9126–9129. DOI: 10.1021/ja303602f

11. Trost, B. M. The Atom Economy—A Search for Synthetic Efficiency. *Science (1979)* **1991**, *254* (5037), 1471–1477. DOI: 10.1126/SCIENCE.1962206.

12. (a) Li, S.; Yang, Q.; Bian, Z.; Wang, J. Rhodium-Catalyzed Enantioselective Hydroselenation of Heterobicyclic Alkenes. *Org. Lett.* **2020**, *22* (7), 2781–2785. DOI: 10.1021/ACS.ORGLETT.0C00762 (b) Ogawa, A.; Kudo, A.; Hirao, T. Palladium-Catalyzed Hydroselenation of Allenes with Benzeneselenol. *Tetrahedron Lett.* **1998**, *39* (29), 5213–5216. DOI: 10.1016/S0040-4039(98)01024-7 (c) Tamai, T.; Yoshikawa, M.; Higashimae, S.; Nomoto, A.; Ogawa, A. Palladium-Catalyzed Markovnikov-Selective Hydroselenation of N-Vinyl Lactams with Selenols Affording N,Se-Acetals. *J. Org. Chem.* **2016**, *81* (1), 324–329. DOI: 10.1021/ACS.JOC.5B02431 (d) Tian, H.; Zhang, H.-M.; Yin, L. Copper(I)-Catalyzed Conjugate Addition/Enantioselective Protonation with Selenols and α-Substituted α,β-Unsaturated Thioamides. *Angew. Chem. Int. Ed.* **2023**, *62* (24), e202301422. DOI: 10.1002/anie.202301422 (e) Slocumb, H. S.; Nie, S.; Dong, V. M.; Yang, X. H. Enantioselective Selenol-Ene Using Rh-Hydride Catalysis. *J. Am. Chem. Soc.* **2022**, *144* (40), 18246–18250. DOI: 10.1021/JACS.2C08475 (f) Kawaguchi, S. I.; Kotani, M.; Atobe, S.; Nomoto, A.; Sonoda, M.; Ogawa, A. Rhodium-Catalyzed Highly Stereoselective Hydroselenation of Internal Alkynes Bearing an Electron-Withdrawing Group. *Organometallics* **2011**, *30* (24), 6766–6769. DOI: 10.1021/OM200663K (g) Ananikov, V. P.; Malyshev, D. A.; Beletskaya, I. P.; Aleksandrov, G. G.; Eremenko, I. L. Palladium and Platinum Catalyzed Hydroselenation of Alkynes: Se–H vs Se–Se Addition to C–C Bond. *J. Organomet. Chem.* **2003**, *679* (2), 162–172. DOI: 10.1016/S0022-328X(03)00546-1. For select reviews: (h) Ishii, A.; Nakata, N. The Mechanism for Transition-Metal-Catalyzed Hydrochalcogenation of Unsaturated Organic Molecules. In *Hydrofunctionalization*, Vol. 43;, Ananikov, V., Tanaka, M., Ed.; Springer, 2011, 21–50. DOI: 10.1007/3418_2011_16 (i) Ogawa, A. Transition-Metal-Catalyzed S–H and Se–H Bonds Addition to Unsaturated Molecules. In *Hydrofunctionalization*, Vol. 43;, Ananikov, V., Tanaka, M., Ed.; Springer, 2011, 325–360. DOI: 10.1007/3418_2011_19

13. Kobiki, Y.; Kawaguchi, S. I.; Ogawa, A. Highly Regioselective Hydroselenation of Inactivated Terminal Alkynes Using Diselenide–$Ph_2P(O)H$ Mixed Systems under Visible-Light Irradiation. *Tetrahedron Lett.* **2013**, *54* (40), 5453–5456. DOI: 10.1016/J.TETLET.2013.07.127.

14. (a) Ogawa, A.; Yokoyama, H.; Yokoyama, K.; Masawaki, T.; Kambe, N.; Sonoda, N. Photoinitiated Addition of Diphenyl Diselenide to Acetylenes. *J. Org. Chem.* **1991**, *56* (19), 5721–5723. DOI: 10.1021/jo00019a052 (b) Patil, D. V.; Hong, Y. T.; Kim, H. Y.; Oh, K. Visible-Light-Induced Three-Component Selenofunctionalization of Alkenes: An Aerobic Selenol Oxidation Approach. *Org. Lett.* **2022**, *24* (46), 8465–8469. DOI: 10.1021/ACS.ORGLETT.2C03186 (c) Chen, J.; Chen, R.; Mei, L.; Yan, S.; Wu, Y.; Li, Q.; Yuan, B. Visible-Light-Induced Difunctionalization of Styrenes: An Efficient and Green Protocol for the Synthesis of β-Acyloxyselenides. *Asian J. Org. Chem.* **2020**, *9* (2), 181–184. DOI: 10.1002/AJOC.201900676 (d) Liu, G. Q.; Zhou, C. F.; Zhang, Y. Q.; Yi, W.; Wang, P. F.; Liu, J.; Ling, Y. Visible-Light-Induced Intermolecular Aminoselenation of Alkenes. *Green Chem.* **2021**, *23* (24), 9968–9973. DOI: 10.1039/D1GC03195C

15. (a) Ye, Z. P.; Xia, P. J.; Liu, F.; Hu, Y. Z.; Song, D.; Xiao, J. A.; Huang, P.; Xiang, H. Y.; Chen, X. Q.; Yang, H. Visible-Light-Induced, Catalyst-Free Radical Cross-Coupling Cyclization of N-Allylbromodifluoroacetamides with Disulfides or Diselenides. *J. Org. Chem.* **2020**, *85* (8), 5670–5682. DOI: 10.1021/ACS.JOC.9B03490 (b) Rathore, V.; Kumar, S. Visible-Light-Induced Metal and Reagent-Free Oxidative Coupling of Sp^2 C–H Bonds with Organo-Dichalcogenides: Synthesis of 3-Organochalcogenyl Indoles. *Green Chem.* **2019**, *21* (10), 2670–2676. DOI: 10.1039/C9GC00007K. (d) Zhang, Q. B.; Ban, Y. L.; Yuan, P. F.; Peng, S. J.; Fang, J. G.; Wu, L. Z.; Liu, Q. Visible-Light-Mediated Aerobic Selenation of (Hetero)Arenes with Diselenides. *Green Chem.* **2017**, *19* (23), 5559–5563. DOI: 10.1039/C7GC02803B

16. (a) Zhou, X. J.; Liu, H. Y.; Mo, Z. Y.; Ma, X. L.; Chen, Y. Y.; Tang, H. T.; Pan, Y. M.; Xu, Y. L. Visible-Light-Promoted Selenylative Spirocyclization of Indolyl-Ynones toward the Formation of 3-Selenospiroindolenine Anticancer Agents. *Chem. Asian J.* **2020**, *15* (10), 1536–1539. DOI: 10.1002/ASIA.202000298 (b) Sahoo, H.; Grandhi, G. S.; Ramakrishna, I.; Baidya, M. Metal-Free Switchable Ortho/Ipso-Cyclization of N-Aryl Alkynamides: Divergent Synthesis of 3-Selenyl Quinolin-2-Ones and Azaspiro[4,5]Trienones. *Org. Biomol. Chem.* **2019**, *17* (48), 10163–10166. DOI: 10.1039/C9OB02177A (c) Ma, X. L.; Wang, Q.; Feng, X. Y.; Mo, Z. Y.; Pan, Y. M.; Chen, Y. Y.; Xin, M.; Xu, Y. L. Metal-Free Visible-Light Induced Cyclization/Substitution Cascade Reaction of Alkyne-Tethered Cyclohexadienones and Diselenides: Access to 5-Hydroxy-3-Selenyl-4a,8a-Dihydro-2H-Chromen-6(5H)-Ones. *Green Chem.* **2019**, *21* (13), 3547–3551. DOI: 10.1039/C9GC00570F (d) Hou, H.; Sun, Y.; Pan, Y.; Yu, H.; Han, Y.; Shi, Y.; Yan, C.; Zhu, S. Visible-Light Mediated Diarylselenylative Cyclization of 1,6-Enynes. *J. Org. Chem.* **2021**, *86* (1), 1273–1280. DOI: 10.1021/ACS.JOC.0C02529 (e) Tran, C. C.; Kawaguchi, S. I.; Sato, F.; Nomoto, A.; Ogawa, A. Photoinduced Cyclizations of O-Diisocyanoarenes with Organic Diselenides and Thiols That Afford Chalcogenated Quinoxalines. *J. Org. Chem.* **2020**, *85* (11), 7258–7266. DOI: 10.1021/ACS.JOC.0C00647 (f) Shi, Q.; Li, P.; Zhang, Y.; Wang, L. Visible Light-Induced Tandem Oxidative Cyclization of 2-Alkynylanilines with Disulfides (Diselenides) to 3-Sulfenyl- and 3-Selenylindoles under Transition Metal-Free and Photocatalyst-Free Conditions. *Org. Chem. Front.* **2017**, *4* (7), 1322–1330. DOI: 10.1039/C7QO00152E (g) Tan, P.; Lu, L.; Wang, S.; Wang, J.; Chen, J.; Zhang, Y.; Xie, L.; Yang, S.; Chen, J.; Zhang, Z. Photo- or Electrochemical Cyclization of Dienes with Diselenides to Access Seleno-Benzo[b]Azepines. *J. Org. Chem.* **2023**, *88* (11), 7245–7255. DOI: 10.1021/ACS.JOC.3C00475

17. (a) Sun, L.; Wang, L.; Alhumade, H.; Yi, H.; Cai, H.; Lei, A. Electrochemical Radical Selenylation of Alkenes and Arenes via Se-Se Bond Activation. *Org. Lett.* **2021**, *23* (20), 7724–7729. DOI: 10.1021/ACS.ORGLETT.1C02661(b) Sun, L.; Yuan, Y.; Yao, M.; Wang, H.; Wang, D.; Gao, M.; Chen, Y. H.; Lei, A. Electrochemical Aminoselenation and Oxyselenation of Styrenes with Hydrogen Evolution. *Org. Lett.* **2019**, *21* (5), 1297–1300. DOI: 10.1021/ACS.ORGLETT.8B03274 (c) Wu, S. F.; Yu, Y.; Yuan, Y.; Li, Z.; Ye, K. Y. Electrochemical Synthesis of β-Fluoroselenides. *Eur. J. Org. Chem.* **2022**, *2022* (41), e202201032. DOI: 10.1002/EJOC.202201032 (d) Liu, G. Q.; Yi, W.; Wang, P. F.; Liu, J.; Ma, M.; Hao, D. Y.; Ming, L.; Ling, Y. Visible-Light-Induced Oxidative Coupling of Vinylarenes with Diselenides Leading to α-Aryl and α-Alkyl Selenomethyl Ketones. *Green Chem.* **2021**, *23* (4), 1840–1846. DOI: 10.1039/D1GC00049G (e) Cui, F. H.; Hua, Y.; Lin, Y. M.; Fei, J.; Gao, L. H.; Zhao, X.; Xia, H. Selective

Difunctionalization of Unactivated Aliphatic Alkenes Enabled by a Metal-Metallaaromatic Catalytic System. *J. Am. Chem. Soc.* **2022**, *144* (5), 2301–2310. DOI: 10.1021/JACS.1C12586 (f) Ito, O. Kinetic Study for Reactions of Phenylseleno Radical with Vinyl Monomers. *J. Am. Chem. Soc.* **1983**, *105*, 850–853. DOI: 10.1021/ja00342a034 (g) Huang, B.; Li, Y.; Yang, C.; Xia, W. Three-Component Aminoselenation of Alkenes via Visible-Light Enabled Fe-Catalysis. *Green Chem.* **2020**, *22* (9), 2804–2809. DOI: 10.1039/C9GC04163J (h) Yin, Y.; Li, C.; Sun, K.; Liu, Y.; Wang, X. Radical Aminoselenation of Styrenes: Facile Access to β-Amido-Selenides. *Chinese J. Org. Chem.* **2022**, *42* (5), 1431–1437. DOI: 10.6023/CJOC202112028 (i) Xu, C.; He, Z.; Kang, X.; Zeng, Q. Highly Selective Radical Isothiocyano-Chalcogenization of Alkenes with NH_4SCN in Water. *Green Chem.* **2021**, *23* (19), 7544–7548. DOI: 10.1039/D1GC02021H (j) Chen, H.; Chen, L.; He, Z.; Zeng, Q. Blue Light-Promoted Radical Sulfoximido-Chalcogenization of Aliphatic and Aromatic Alkenes. *Green Chem.* **2021**, *23* (7), 2624–2627. DOI: 10.1039/D0GC03899G (k) Sun, K.; Wang, X.; Lv, Y.; Li, G.; Jiao, H.; Dai, C.; Li, Y.; Zhang, C.; Liu, L. Peroxodisulfate-Mediated Selenoamination of Alkenes Yielding Amidoselenide-Containing Sulfamides and Azoles. *Chem. Comm.* **2016**, *52* (54), 8471–8474. DOI: 10.1039/C6CC04225B (l) Giese, B. Formation of CC Bonds by Addition of Free Radicals to Alkenes. *Angew. Chem. Int. Ed.* **1983**, *22* (10), 753–764. DOI: 10.1002/ANIE.198307531

18. Sonoda, N.; Ogawa, A.; Recupero, F. Benzeneselenol. *Encyclopedia of Reagents for Organic Synthesis* **2005**, 1–7. DOI: 10.1002/047084289X.RB018.PUB2

19. Pitzer, L.; Schäfers, F.; Glorius, F. Rapid Assessment of the Reaction-Condition-Based Sensitivity of Chemical Transformations. *Angew. Chem. Int. Ed.* **2019**, *58* (25), 8572–8576. DOI: 10.1002/anie.201901935

20. Srinivas, B.; Kumar, V. P.; Sridhar, R.; Reddy, V. P.; Nageswar, Y. V. D.; Rao, K. R. β-Cyclodextrin-Promoted Addition of Benzeneselenol to Conjugated Alkenes in Water. *Helv. Chim. Acta* **2009**, *92* (6), 1080–1084. DOI: 10.1002/HLCA.200800378

21. Ushakov, S. N.; A. M. Itenberg. The Synthesis of Triethylvinylsilicane. *Zh. Obshch. Khim* **1937**, *7*, 2495–2498.

22. For select reviews, see: (a) Roberts, D. D.; McLaughlin, M. G. Strategic Applications of the β-Silicon Effect. *Adv. Synth. Catal.* **2022**, *364* (14), 2307–2332. DOI: 10.1002/ADSC.202200237 (b) Lambert, J. B.; Zhao, Y.; Emblidge, R. W.; Salvador, L. A.; Liu, X.; So, J. H.; Chelius, E. C. The β Effect of Silicon and Related Manifestations of σ Conjugation. *Acc. Chem. Res.* **1999**, *32* (2), 183–190. DOI: 10.1021/ar970296m

23. For select reviews, see: (a) Lu, L.; Huang, D.; Wang, Z.; Wang, X.; Wu, X. Recent Developments in Selenylation and Thiolation of Alkenes via Three-Component Reactions. *Adv. Synth. Cata.l* **2023**, *365* (14), 2310–2331. DOI: 10.1002/ADSC.202300434 (b) Maji, B. Stereoselective Haliranium, Thiiranium and Seleniranium Ion-Triggered Friedel–Crafts-Type Alkylations for Polyene Cyclizations. *Adv. Synth. Catal.* **2019**, *361* (15), 3453–3489. DOI: 10.1002/ADSC.201900028 (c) Potapov, V.A.; Musalov, M.V.; Musalova, M.V.; Amosova, S.V. Recent Advances in Organochalcogen Synthesis Based on Reactions of Chalcogen Halides with Alkynes and Alkenes. *Curr. Org. Chem.* **2016** *20* (2), 136–145. DOI: 10.2174/1385272819666150810222454

24. (a) Zhang, H.; Lin, S.; Jacobsen, E. N. Enantioselective Selenocyclization via Dynamic Kinetic Resolution of Seleniranium Ions by Hydrogen-Bond Donor Catalysts. *J. Am. Chem. Soc.* **2014**, *136* (47), 16485–16488. DOI: 10.1021/JA510113S (b) Denmark, S. E.; Kalyani, D.; Collins, W. R. Preparative and Mechanistic Studies toward the Rational Development of Catalytic, Enantioselective Selenoetherification Reactions. *J. Am. Chem. Soc.* **2010**, *132* (44), 15752–15765. DOI: 10.1021/JA106837B (c) See, J. Y.; Yang, H.; Zhao, Y.; Wong, M. W.; Ke, Z.; Yeung, Y. Y. Desymmetrizing Enantio- and Diastereoselective Selenoetherification through Supramolecular Catalysis. *ACS Catal*. **2018**, *8* (2), 850–858. DOI: 10.1021/ACSCATAL.7B03510

25. (a) Clive, D. L. J.; Chittattu, G. New Route to Bicyclic Lactones: Use of Benzeneselenenyl Chloride. *J. Chem. Soc. Chem. Commun*. **1977**, *14*, 484–485. DOI: 10.1039/C39770000484 (b)Nicolaou, K. C.; Lysenko, Z. Phenylselenolactonization. An Extremely Mild and Synthetically Useful Cyclization Process. *J Am Chem Soc* **1977**, *99* (9), 3185–3187. DOI: 10.1021/JA00451A065 (c) Nicolaou, K. C.; Seitz, S. P.; Sipio, W. J.; Blount, J. F. Phenylseleno- and Phenylsulfenolactonizations. Two Highly Efficient and Synthetically Useful Cyclization Procedures. *J. Am. Chem. Soc.* **1979**, *101* (14), 3884–3893. DOI: 10.1021/JA00508A028 (d) Clive, D. L. J.; Russell, C. G.; Chittattu, G.; Singh, A. Cyclofunctionalisation of Unsaturated Acids with Benzeneselenenyl Chloride : Kinetic and Thermodynamic Aspects of the Rules for Ring Closure. *Tetrahedron* **1980**, *36* (10), 1399–1408. DOI: 10.1016/0040-4020(80)85054-X (e) Denmark, S. E.; Edwards, M. G. On the Mechanism of the Selenolactonization Reaction with Selenenyl Halides. *J. Org. Chem.* **2006**, *71* (19), 7293–7306. DOI: 10.1021/JO0610457 (f) Niu, W.; Yeung, Y. Y. Catalytic and Highly Enantioselective Selenolactonization. *Org. Lett.* **2015**, *17* (7), 1660–1663. DOI: 10.1021/ACS.ORGLETT.5B00377

26. (a) Denmark, S. E.; Collins, W. R.; Cullen, M. D. Observation of Direct Sulfenium and Selenenium Group Transfer from Thiiranium and Seleniranium Ions to Alkenes. *J. Am. Chem. Soc.* **2009**, *131* (10), 3490–3492. DOI: 10.1021/JA900187Y (b) Poleschner, H.; Seppelt, K. Seleniranium and Telluriranium Salts. *Chem. Eur. J.* **2018**, *24* (64), 17155–17161. DOI: 10.1002/CHEM.201804307 (c) Bock, J.; Daniliuc, C. G.; Bergander, K.; Mück-Lichtenfeld, C.; Hennecke, U. Synthesis, Structural Characterisation, and Synthetic Application of Stable Seleniranium Ions. *Org. Biomol. Chem.* **2019**, *17* (12), 3181–3185. DOI: https://doi.org/10.1039/C9OB00078J

27. (a) Luo, X.; Tang, X.; Ni, J.; Wu, B.; Li, C.; Shao, M.; Wei, Z. Electrochemical Oxidation of Styrene to Benzaldehyde by Discrimination of Spin-Paired π Electrons. *Chem. Sci.* **2023**, *14* (7), 1679–1686. DOI: 10.1039/D2SC05913D (b) Ren, S. Y.; Zhou, Q.; Zhou, H. Y.; Wang, L. W.; Mulina, O. M.; Paveliev, S. A.; Tang, H. T.; Terent'ev, A. O.; Pan, Y. M.; Meng, X. J. Three-Component Electrochemical Aminoselenation of 1,3-Dienes. *J. Org. Chem.* **2023**, *88* (9), 5760–5771. DOI: 10.1021/acs.joc.3c00214

28. Marcus, R. A. On the Theory of Oxidation-Reduction Reactions Involving Electron Transfer. I. *J. Chem. Phys.* **1956**, *24* (5), 966–978. DOI: 10.1063/1.1742723.

29. For select reviews, see: (a) Crossley, S. W. M.; Obradors, C.; Martinez, R. M.; Shenvi, R. A. Mn-, Fe-, and Co-Catalyzed Radical Hydrofunctionalizations of Olefins. *Chem. Rev.* **2016**, *116* (15), 8912–9000. DOI: 10.1021/ACS.CHEMREV.6B00334/ (b) Shevick, S. L.; Wilson, C. V.; Kotesova, S.; Kim, D.; Holland, P. L.; Shenvi, R. A. Catalytic Hydrogen Atom Transfer to Alkenes: A Roadmap for Metal Hydrides and Radicals. *Chem. Sci.* **2020**, *11* (46), 12401–12422. DOI: 10.1039/D0SC04112B (c) Shenvi, R. A.; Matos, J. L. M.; Green, S. A. Hydrofunctionalization of Alkenes by Hydrogen-Atom Transfer. *Org. Reactions* **2019**, *100*, 383–470. DOI: 10.1002/0471264180.OR100.07. For the seminal work on MHAT, see: Lo, J. C.; Gui, J.; Yabe, Y.; Pan, C. M.; Baran, P. S. Functionalized Olefin Cross-Coupling to Construct Carbon–Carbon Bonds. *Nature* **2014**, *516* (7531), 343–348. DOI: 10.1038/nature14006.

30. For a review, see: (a) Margrey, K. A.; Nicewicz, D. A. A General Approach to Catalytic Alkene Anti-Markovnikov Hydrofunctionalization Reactions via Acridinium Photoredox Catalysis. *Acc. Chem. Res.* **2016**, *49* (9), 1997–2006. DOI: 10.1021/ACS.ACCOUNTS.6B00304. For select examples, see: (b) Wilger, D. J.; Grandjean, J. M. M.; Lammert, T. R.; Nicewicz, D. A. The Direct Anti-Markovnikov Addition of Mineral Acids to Styrenes. *Nat. Chem.* **2014**, *6* (8), 720–726. DOI: 10.1038/nchem.2000 (c) Nguyen, T. M.; Nicewicz, D. A. Anti-Markovnikov Hydroamination of Alkenes Catalyzed by an Organic Photoredox System. *J. Am. Chem. Soc.* **2013**, *135* (26), 9588–9591. DOI: 10.1021/JA4031616 (d) Romero, N. A.; Nicewicz, D. A. Mechanistic Insight into the Photoredox Catalysis of Anti-Markovnikov Alkene Hydrofunctionalization Reactions. *J Am Chem Soc* **2014**, *136* (49), 17024–17035. DOI: 10.1021/JA506228U/

31. For select reviews, see: (a) Sinha, A. K.; Equbal, D. Thiol−Ene Reaction: Synthetic Aspects and Mechanistic Studies of an Anti-Markovnikov-Selective Hydrothiolation of Olefins. *Asian J. Org. Chem.* **2019**, *8* (1), 32–47. DOI: 10.1002/AJOC.201800639 (b) Hoyle, C. E.; Lowe, A. B.; Bowman, C. N. Thiol-Click Chemistry: A Multifaceted Toolbox for Small Molecule and Polymer Synthesis. *Chem. Soc. Rev.* **2010**, *39* (4), 1355–1387. DOI: 10.1039/B901979K. For select examples, see: (c) Posner, T. Beiträge zur Kenntniss der ungesättigten Verbindungen. II. Ueber die Addition von Mercaptanen an ungesättigte Kohlenwasserstoffe. *Ber. Dtsch. Chem. Ges.*, **1905**, *38*, 646–657. DOI: 10.1002/cber.190503801106 (d) Musacchio, A. J.; Lainhart, B. C.; Zhang, X.; Naguib, S. G.; Sherwood, T. C.; Knowles, R. R. Catalytic Intermolecular Hydroaminations of Unactivated Olefins with Secondary Alkyl Amines. *Science* **2017**, *355* (6326), 727–730. DOI: 10.1126/science.aal3010 (e) Xu, E. Y.; Werth, J.; Roos, C. B.; Bendelsmith, A. J.; Sigman, M. S.; Knowles, R. R. Noncovalent Stabilization of Radical Intermediates in the Enantioselective Hydroamination of Alkenes with Sulfonamides. *J. Am. Chem. Soc.* **2022**, *144* (41), 18948–18958. DOI: 10.1021/JACS.2C07099 For a related example, see: (f) Teders, M.; Henkel, C.; Anhäuser, L.; Strieth-Kalthoff, F.; Gómez-Suárez, A.; Kleinmans, R.; Kahnt, A.; Rentmeister, A.; Guldi, D.; Glorius, F. The energy-transfer-enabled biocompatible disulfide-ene reaction. Nat. Chem. 2018, 10, 981–988, DOI: 10.1038/s41557-018-0102-z

32. Franzke, Y. J.; Holzer, C.; Andersen, J. H.; Begušić, T.; Bruder, F.; Coriani, S.; Della Sala, F.; Fabiano, E.; Fedotov, D. A.; Fürst, S.; Gillhuber, S.; Grotjahn, R.; Kaupp, M.; Kehry, M.; Krstić, M.; Mack, F.; Majumdar, S.; Nguyen, B. D.; Parker, S. M.; Pauly, F.; Pausch, A.; Perlt, E.; Phun, G. S.; Rajabi, A.; Rappoport, D.; Samal, B.; Schrader, T.; Sharma, M.; Tapavicza, E.; Treß, R. S.; Voora, V.; Wodyński, A.; Yu, J. M.; Zerulla, B.; Furche, F.; Hättig, C.; Sierka, M.; Tew, D. P.; Weigend, F. TURBOMOLE: Today and Tomorrow. *J. Chem. Theory Comput.* **2023**, *19* (20), 6859–6890. DOI: 10.1021/acs.jctc.3c00347

33. (a) Adamo, C.; Scuseria, G. E.; Barone, V. Accurate Excitation Energies from Time-Dependent Density Functional Theory: Assessing the PBE0 Model. *J. Chem. Phys.* **1999**, *111* (7), 2889–2899. DOI: 10.1063/1.479571 (b) Perdew, J. P.; Ernzerhof, M.; Burke, K. Rationale for Mixing Exact Exchange with Density Functional Approximations. *J. Chem. Phys.* **1996**, *105* (22), 9982–9985. DOI: 10.1063/1.472933.

34. Weigend, F.; Ahlrichs, R. Balanced Basis Sets of Split Valence, Triple Zeta Valence and Quadruple Zeta Valence Quality for H to Rn: Design and Assessment of Accuracy. *Phys. Chem. Chem. Phys.* **2005**, *7* (18), 3297–3305. DOI: 10.1039/B508541A

35. Dunlap, B. I.; Connolly, J. W. D.; Sabin, J. R. On Some Approximations in Applications of Xα Theory. *J. Chem. Phys.* **1979**, *71* (8), 3396–3402. DOI: 10.1063/1.438728

36. Grimme, S.; Antony, J.; Ehrlich, S.; Krieg, H. A Consistent and Accurate Ab Initio Parametrization of Density Functional Dispersion Correction (DFT-D) for the 94 Elements H–Pu. *J. Chem. Phys.* **2010**, *132* (15), 46. DOI: 10.1063/1.3382344/926936

37. Klamt, A.; Schüürmann, G. COSMO: A New Approach to Dielectric Screening in Solvents with Explicit Expressions for the Screening Energy and Its Gradient. *J. Chem. Soc., Perkin Trans. 2* **1993**, *5*, 799–805. DOI: 10.1039/P29930000799

38. (a) Chen, G. P.; Voora, V. K.; Agee, M. M.; Balasubramani, S. G.; Furche, F. Random-Phase Approximation Methods. *Annual Rev. Phys. Chem.* **2017**, *68*, 421–445. DOI: 10.1146/annurev-physchem-040215-112308 (b) Eshuis, H.; Bates, J. E.; Furche, F. Electron Correlation Methods Based on the Random Phase Approximation. *Theor. Chem. Acc.* **2012**, *131* (1), 1–18. DOI: 10.1007/s00214-011-1084-8. (c) Voora, V. K.; Balasubramani, S. G.; Furche, F. Variational Generalized Kohn-Sham Approach Combining the Random-Phase-Approximation and Green's-Function Methods. *Phys. Rev. A* **2019**, *99* (1), 012518. DOI: 10.1103/PhysRevA.99.012518

39. Eshuis, H.; Yarkony, J.; Furche, F. Fast Computation of Molecular Random Phase Approximation Correlation Energies Using Resolution of the Identity and Imaginary Frequency Integration. *J. Chem. Phys.* **2010**, *132* (23), 37. DOI: 10.1063/1.3442749/71464

40. Bannwarth, C.; Caldeweyher, E.; Ehlert, S.; Hansen, A.; Pracht, P.; Seibert, J.; Spicher, S.; Grimme, S. Extended Tight-Binding Quantum Chemistry Methods. *Wiley Interdiscip. Rev. Comput. Mol. Sci.* **2021**, *11* (2), e1493. DOI: 10.1002/WCMS.1493.

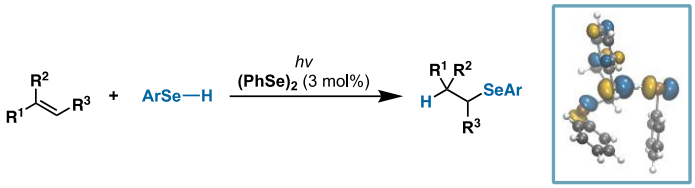

• high *anti*-selectivity • broad substrate scope • identification of β-selenide effect •